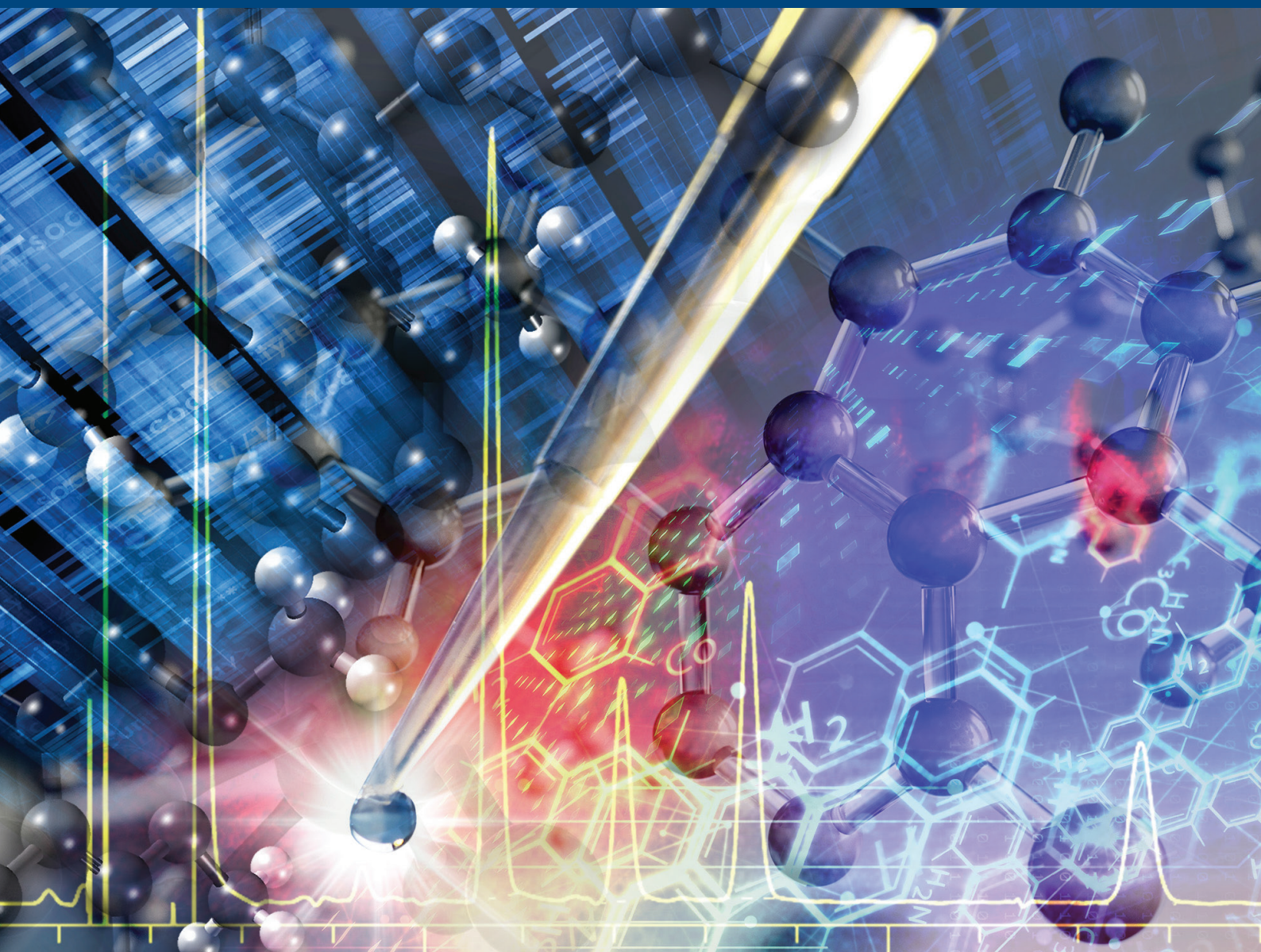


JOURNAL OF SEPARATION SCIENCE

13 | 2021



Methods

Chromatography · Electroseparation

Applications

Biomedicine · Foods · Environment

www.jss-journal.com

WILEY-VCH

RESEARCH ARTICLE

Polymeric metal-containing ionic liquid sorbent coating for the determination of amines using headspace solid-phase microextraction

Kateryna Yavir¹  | Philip Eor² | Adam Kloskowski¹  | Jared L. Anderson² 

¹ Department of Physical Chemistry, Faculty of Chemistry, Gdansk University of Technology, Gdansk, Poland

² Department of Chemistry, Iowa State University, Ames, Iowa, USA

Correspondence

Prof. Jared L. Anderson, Department of Chemistry, Iowa State University, 1605 Gilman Hall, Ames, IA 50011, USA.

Email: andersoj@iastate.edu

This study describes the design, synthesis, and application of polymeric ionic liquid sorbent coatings featuring nickel metal centers for the determination of volatile and semivolatile amines from water samples using headspace solid-phase microextraction. The examined polymeric ionic liquid (PIL) sorbent coatings were composed of two ionic liquid monomers (tetra(3-vinylimidazolium)nickel bis[(trifluoromethyl)sulfonyl]imide $[\text{Ni}^{2+}(\text{VIM})_4] 2[\text{NTf}_2^-]$ and 1-vinyl-3-hexylimidazolium $[\text{HVIM}^+][\text{NTf}_2^-]$), and an ionic liquid cross-linker (1,12-di(3-vinylimidazolium)dodecane $[(\text{VIM})_2\text{C}_{12}^{2+}] 2[\text{NTf}_2^-]$). With these ionic liquid monomers and cross-linkers, three different types of coatings were prepared: PIL 1 based on the neat $[\text{Ni}^{2+}(\text{VIM})_4] 2[\text{NTf}_2^-]$ monomer, PIL 2 consisting of the $[\text{Ni}^{2+}(\text{VIM})_4] 2[\text{NTf}_2^-]$ monomer with addition of cross-linker, and PIL 3 composed of the $[\text{HVIM}^+][\text{NTf}_2^-]$ monomer and cross-linker. Analytical performance of the prepared sorbent coatings using headspace solid-phase microextraction gas chromatography–mass spectrometry was compared with the polydimethylsiloxane and polyacrylate commercial coatings. The PIL 2 sorbent coating yielded the highest enrichment factors ranging from 5500 to over 160 000 for the target analytes. The developed headspace solid-phase microextraction gas chromatography–mass spectrometry method was applied for the analysis of real samples (the concentration of amines was 200 $\mu\text{g/L}$), producing relative recovery values in the range of 90.9–120.0% (PIL 1) and 83.0–122.7% (PIL 2) from tap water, and 84.8–112.4% (PIL 1) and 79.2–119.3% (PIL 2) from lake water.

KEYWORDS

amines, nickel, polymeric ionic liquids, solid-phase microextraction

1 | INTRODUCTION

Amines are well-known environmental pollutants that are widespread throughout the world. They can be released from a variety of anthropogenic (chemicals, pesticides, pharmaceuticals, automobiles, dyestuff, etc.) and natural

Article Related Abbreviations: 2,6-DTBP, 2,6-di-tert-butylpyridine; EF, enrichment factor; HS, headspace; IL, ionic liquid; MCIL, metal-containing ionic liquid; PA, polyacrylate; PDMS, polydimethylsiloxane; PIL, polymeric ionic liquid; RR, relative recovery

This is an open access article under the terms of the [Creative Commons Attribution](https://creativecommons.org/licenses/by/4.0/) License, which permits use, distribution and reproduction in any medium, provided the original work is properly cited.

© 2021 The Authors. *Journal of Separation Science* published by Wiley-VCH GmbH

sources (biomass burning, oceans, and vegetation) [1]. Amines are easily released to the environment through groundwater, rivers, lakes, and soil as well as industrial effluents or chemical decomposition products [2]. Most compounds of this class are hazardous and toxic to humans and animals. They can react with nitrosylating agents and, as a consequence, be converted to carcinogenic *N*-nitroamines [3]. Even though contamination of amines can exist in the environment at trace levels, they may have a mutagenic and toxic effect on animals and humans. Therefore, the concentration of amines in the surrounding water must be continuously monitored, and it is vital to find fast, easy, effective, and sensitive methods for their determination.

SPME is a solvent-free extraction technique and is an alternative to conventional extraction methods, such as LLE and SPE [4]. The procedure for extracting analytes from an aqueous solution using SPME consists of the following three main steps: (a) exposing the fiber to the sample by direct-immersion (DI) or the headspace (HS) above the sample, (b) absorbing/adsorbing the analytes by the sorbent, and (c) desorption of the analytes from the coating by thermal or solvent extraction. The SPME method has become widely used to determine a wide range of analytes from complex matrices, such as samples of food products, biological substances, pharmaceuticals, and environmental samples [5–8]. SPME has numerous advantages over other extraction methods, such as being simple, rapid, easily automated, eliminates the use of toxic solvents, and allows for the collection of samples *in situ* and *in vivo*. One of the most important limitations of the method is the choice of commercially available SPME sorbent coatings. Therefore, on-going research in the field is focused on developing new sorbent coatings that extend the range of analytes that can be effectively extracted. Various materials such as nanoparticles of noble metals, sorbents based on silica (silicon dioxide), ionogels, molecularly imprinted polymers, conductive polymers, carbon nanotubes, metal and/or metal oxide nanoparticles, graphene and graphene oxide, metal organic frameworks, ionic liquids (ILs), and polymeric ionic liquids (PILs) [9–17] hold promise due to their desired tunability. The above drawbacks are related to the general limitations of the SPME method. However, in the case of amine determination by SPME coupled to GC, a number of additional problems arise due to their high aqueous solubility, volatility, polarity, and highly basic character (i.e., stronger sorption to polar stationary phases is observed with the decrease in the molecular mass of amines) [18].

ILs are a well-known group of materials that have been used as SPME sorbent coatings. These compounds consist of a bulky organic cation and a smaller inorganic/organic

anion and are present as liquids below 100°C. The physical and chemical properties of ILs are highly tunable based on selecting an appropriate anion and cation pair. When ILs are used as a polymerizable monomer, PILs are formed and retain many of the unique physicochemical properties of ILs as well as additional advantages that include higher thermal and chemical stability, and a negligible change in viscosity when subjected to high temperatures [19, 20]. PILs have been used for the determination of various classes of analytes, including polycyclic aromatic hydrocarbons, fatty acid methyl esters, esters and benzene derivatives, carbon dioxide, estrogens, alcohols and amines, genotoxic or structurally alerting alkyl halides and aromatics, pyrethroids, and contaminants of emerging concern [10, 11, 21].

Another interesting subclass of ILs is metal-containing ionic liquids (MCILs). MCILs are formed by incorporating transition and/or rare earth metals into their chemical structure [22]. In addition to possessing fundamental properties of ILs, the paramagnetic metals in MCILs impart magnetic, catalytic, and optical properties, which significantly increases the scope of their applications [23, 24]. MCILs have been used in various areas of analytical chemistry including extractions and microextractions, chromatographic separations, membrane applications and gas absorption, electrochemistry, and sensors [25, 26]. Incorporation of metal ions (Ni^{2+} , Mn^{2+} , Co^{2+} , Dy^{3+} , Gd^{3+} , Nd^{3+}) into the IL chemical structure significantly influences their interactions with analytes originating from different organic subclasses such as alcohols, ketones, chlorinated alkanes, aromatic compounds, and amines [22, 27]. It has been observed that nickel-containing MCILs exhibit unique selectivity toward amines [27]. The viscosity of MCILs drops significantly with an increase in temperature, rendering them impractical in SPME. To overcome this obstacle, the creation of a polymerizable sorbent coating is required. A procedure using vinylimidazole ligands coordinated to silver ion and subsequent free radical polymerization to form a polymeric MCIL was previously reported [28].

Using this approach, nickel-based PILs were synthesized in this study with or without the addition of cross-linker to investigate its effect on amine extraction performance. According to a previous study by Ho et al. [29], cross-linked PILs possess higher durability, stability, and robustness compared to linear PIL-based coatings. The effect of nickel cation in the PIL chemical structure was studied by further comparing the extraction performance to a structurally similar PIL coating lacking the metal center. To benchmark the sorbent coatings, extractions of the targeted amine analytes were compared to commercially available fibers consisting of polydimethylsiloxane

(PDMS) and polyacrylate (PA) sorbent coatings. The developed HS-SPME-GC-MS method was finally applied for the analysis of real samples, including tap and lake water.

2 | MATERIALS AND METHODS

2.1 | Reagents and materials

The group of studied amines included pyridine (99.8%), triallylamine (99.0%), tripropylamine ($\geq 98.0\%$), 3-ethylpyridine ($\geq 98.0\%$), aniline (99.5%), and 2,6-di-tert-butylpyridine (2,6-DTBP, $\geq 97.0\%$), all purchased from Sigma-Aldrich (St. Louis, MO, USA). Supporting Information Table S1 shows the structures and various physicochemical properties of the analytes. Stock solutions of the individual analytes were prepared in acetonitrile (99.8%; Sigma-Aldrich) at a concentration of 2000 mg/L. The intermediate solutions in acetonitrile were prepared by diluting the set of individual stock solutions to a level of 100 mg/L for each analyte. GC-MS calibration curves were obtained using a set of solutions prepared so that the volume of injected standard solutions was equal to 1 μL . Working solutions were prepared by spiking the intermediate solution into the ultrapure or real water samples containing sodium chloride (NaCl, $\geq 99.5\%$, purchased from Fisher Scientific, Fair Lawn, NJ, USA). Ultrapure water (18.2 M Ω cm) was obtained from a Milli-Q water purification system (Millipore, Bedford, MA, USA).

For the synthesis of monomers and cross-linkers, the following reagents were used: 1-vinylimidazole ($\geq 99.0\%$), nickel(II) chloride (98.0%), 1,12-dibromododecane (98.0%), and 1-bromohexane (98.0%), all purchased from Sigma-Aldrich. Lithium bis[(trifluoromethyl)sulfonyl]imide (LiNTf₂) was acquired from SynQuest Laboratories (Alachua, FL, USA). The reagent 2-hydroxy-2-methylpropiophenone ($>96.0\%$, DAROCUR 1173; Sigma-Aldrich) was used as an initiator in the polymerization reaction. Methanol (99.8%), ethyl acetate (99.8%), isopropanol (99.5%), and dichloromethane ($\geq 99.8\%$) were purchased from Sigma-Aldrich.

The commercial SPME fibers, featuring PA (85 μm) and PDMS (100 μm) coatings, were provided as gifts from Millipore-Sigma. Elastic nitinol wires were used as solid supports in the preparation of the SPME fibers (Nitinol Devices & Components, Fremont, CA, USA). Blank SPME assemblies (24 Ga) were provided by Millipore-Sigma (Bellefonte, PA, USA).

Real water samples were collected from the laboratory tap in Ames (IA, USA) and from Lake LaVerne on the campus of Iowa State University, respectively. The samples were stored in the dark using glass bottles at 4°C before

use. Prior to analysis, NaCl was added to a concentration of 30% (w/v).

2.2 | Instrumentation

Amine separations were carried out using an Agilent Technologies 7890B GC equipped with a 5977A MS detector (single quadrupole) on a CP-Sil8 CB capillary column (length 30 m, 0.25 mm ID, 0.25 μm film thickness). Ultrapure helium was used as carrier gas at a flow rate of 1 mL/min. The inlet was operated in splitless mode with an inlet temperature of 190°C. The following oven program was used: initial temperature equal to 40°C, then the temperature was increased at 2°C/min up to 80°C, followed by an increase to 270°C at 30°C/min, and finally held for 1 min. The MS employed electron ionization (EI) at 70 eV and gain factor mode. The transfer line temperature was set at 250°C, while the source and quadrupole temperatures were fixed at 230 and 150°C, respectively. Data were acquired in single ion monitoring mode. Identification of the amines was accomplished by considering the retention time, presence of quantifier and qualifier ions for each analyte (see Supporting Information Table S1), and the ratio between those ions. The peak area corresponding to the quantifier ion was used for quantitative purposes.

Scanning electron microscopy (SEM) images of the nickel-based PIL fibers were obtained using a FEI Quanta-250 microscope (FE-SEM).

2.3 | Synthesis of IL monomers and cross-linker

Two IL monomers, namely, 1-vinyl-3-hexylimidazolium bis[(trifluoromethyl)sulfonyl]imide [HVIM⁺][NTf₂⁻] and tetra(3-vinylimidazolium)nickel bis[(trifluoromethyl)sulfonyl]imide [Ni²⁺(VIM)₄] 2[NTf₂⁻], as well as the 1,12-di(3-vinylimidazolium) dodecane bis[(trifluoromethyl)sulfonyl]imide [(VIM)₂C₁₂²⁺] 2[NTf₂⁻] IL cross-linker were synthesized and used in the study.

The [Ni²⁺(VIM)₄] 2[NTf₂⁻] IL monomer was synthesized using a modification of a previously published procedure [26]. One equivalent (millimolar) of anhydrous nickel (II) chloride was added to four equivalents of 1-vinylimidazole in methanol with stirring at room temperature overnight. After reaction, solvent was removed by rotary evaporation. The resulting solid material was dried under vacuum for 24 h at 40°C. The obtained solid ([Ni²⁺(VIM)₄] 2[Cl⁻]) was then reacted with LiNTf₂ at a 1:4 molar ratio, respectively, in acetone and water by stirring at room temperature for 5 h. The solvent was subsequently evaporated and the material dried under vacuum. After

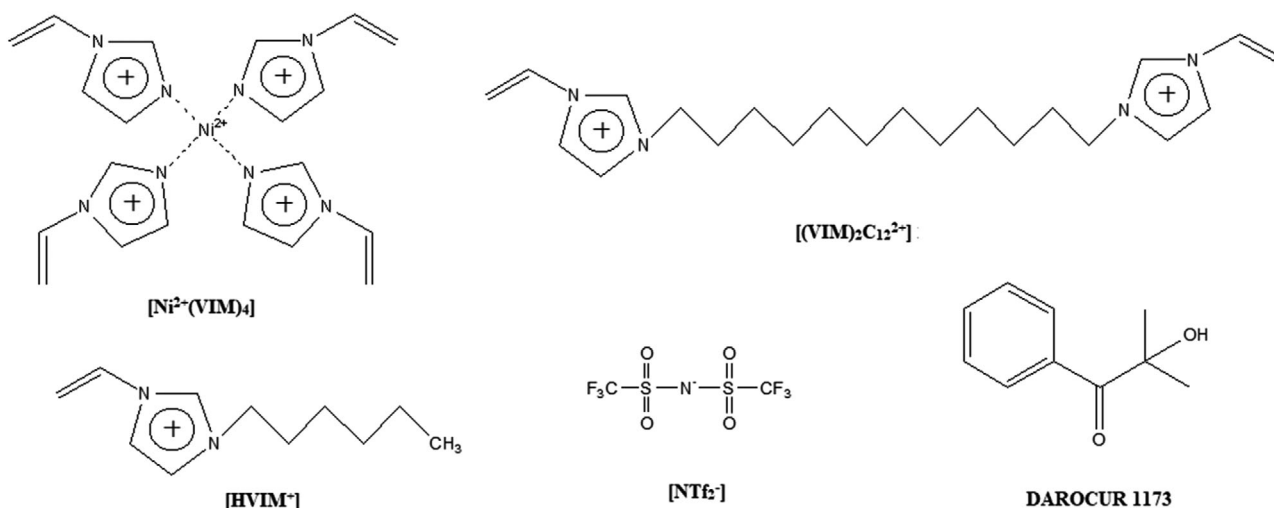
TABLE 1 Composition of sorbent coatings and dimensions of fibers examined in this study

PIL fiber abbreviation ^a	IL monomer	IL cross-linker ^b	Film thickness ± SD (μm) ^c	Volume (μL)
PIL 1	[Ni ²⁺ (VIM) ₄] 2[NTf ₂ ⁻]	–	~8 ± 1.3	0.043
PIL 2	[Ni ²⁺ (VIM) ₄] 2[NTf ₂ ⁻]	[(VIM) ₂ C ₁₂ ²⁺] 2[NTf ₂ ⁻]	~11 ± 1.9	0.063
PIL 3	[HVIM ⁺][NTf ₂ ⁻]	[(VIM) ₂ C ₁₂ ²⁺] 2[NTf ₂ ⁻]	~22 ± 3.8	0.146

^aDAROCUR 1173 was used as a UV initiator for all fibers (50% w/w, respect to the monomer).

^b50% w/w, respect to the monomer.

^cEstimated from SEM images (the length of fibers were 1.35 cm).

**FIGURE 1** Chemical structures of the cations, anion, and UV initiator (DAROCUR 1173) used for the preparation of sorbent coatings investigated in this study

drying, the material was dissolved in dichloromethane, and remaining lithium chloride was removed by LLE with ultrapure water. In the final step, dichloromethane was evaporated under vacuum for 24 h at 40°C. Elemental analysis (CHN): calculated % for C₂₄H₂₄F₁₂N₁₀NiO₈S₄, calculated; C, 28.96; H, 2.43; N, 14.07; S, 12.88. Found; C, 34.56; H, 3.17; N, 13.85; S, 9.34.

The [HVIM⁺][NTf₂⁻] IL monomer and [(VIM)₂C₁₂²⁺] 2[NTf₂⁻] IL cross-linker were synthesized according to previously published methods [30, 31]. The monomer and cross-linker were characterized using ¹H NMR and ESI-MS and spectra are shown in Supporting Information Figures S1–5.

2.4 | Preparation of SPME fibers

All coatings were prepared by on-fiber UV-initiated polymerization following previously described procedures [29]. The composition and mass ratio of components used for the preparation of the IL-based coatings are shown in Table 1 and Figure 1. Three types of coat-

ings were prepared as follows: PIL 1 consisting of pure [Ni²⁺(VIM)₄] 2[NTf₂⁻] monomer; PIL 2 with monomer and [(VIM)₂C₁₂²⁺] 2[NTf₂⁻] cross-linker, and PIL 3 based on the [HVIM⁺][NTf₂⁻] monomer and cross-linker. The PIL3 coating was used as a reference to study the effect of Ni²⁺ metal center in the PIL on extraction performance. The IL monomer, IL cross-linker (if applied), and free radical initiator were mixed in appropriate proportions at 55°C. The homogenous mixture was manually placed on the surface of a previously derivatized nitinol support. Derivatization of elastic nitinol wires was carried out according to a previously published method [32] and glued into a commercial SPME device. The coatings were exposed to UV irradiation (360 nm) for 2 h to promote polymerization. Finally, the obtained fibers were thermally conditioned in the GC injection port at 200°C for 30 min.

2.5 | HS-SPME procedure

Samples for HS-SPME were placed in 20-mL glass vials closed with open-top caps and polytetrafluoroethylene/

silicone septa (Supelco). For all experiments, the sample volume was maintained at 10 mL. Before exposure of the SPME fiber, samples were thermostated at the temperature of extraction for 15 min using a hotplate with an accuracy of $\pm 0.5^\circ\text{C}$. Subsequently, samples were spiked with required volumes of the stock solution and mixed at 800 rpm for 5 min. A Corning PC-420D magnetic stirring hotplate (Corning, NY, USA) and a stir bar (1 cm length \times 0.5 cm diameter; Fisher Scientific) were used for mixing. The fiber was exposed to the HS of the sample solution for 10–70 min at 25–70°C. After extraction, the fibers were immediately inserted into the GC injection port for thermal desorption at 190°C for 10 min. The temperature and desorption time were optimized in advance by studying carry-over effects.

The amino functional groups within amine molecules are responsible for strong and specific interactions with silane groups and siloxane bridges. Consequently, this leads to their strong retention, which often results in broad, asymmetrical chromatographic peaks and low sensitivity. To avoid these issues, it is necessary to choose an optimal GC column. The following capillary columns were examined to identify the most effective separation of amines: HP-5 ms (30 m, 0.25 mm ID, 0.25 μm film thickness), DB-WAX (30 m, 0.25 mm ID, 0.25 μm film thickness), and CP-Sil8 CB (30 m, 0.25 mm ID, 0.25 μm film thickness). The CP-Sil8 CB column has demonstrated superior performance in amine separation and was selected for further studies.

3 | RESULTS AND DISCUSSION

3.1 | Characterization of nickel-based polymeric IL fibers

The introduction of transition metals into the IL chemical structure may significantly affect its interactions with organic compounds, thereby influencing extraction properties. This feature was exploited in the determination of phenolics, polycyclic aromatic hydrocarbon, insecticide compounds, and lipophilic organic UV filters using MCILs in micro-liquid extraction techniques [33, 34]. More systematic studies evaluating the selectivity of MCILs were performed by studying the retention of analytes obtained from inverse gas chromatography when the MCIL is used as a stationary phase [27]. MCILs with anions containing metals (Ni^{2+} , Mn^{2+} , Co^{2+} , Dy^{3+} , Gd^{3+} , Nd^{3+}) with acetylacetonate ligands were investigated. The results indicated an exceptionally high affinity of amines (especially pyridine) for nickel-containing MCILs. However, due to their liquid state, these compounds cannot be directly applied as extraction phases in SPME. In this study, the struc-

tural features of the MCIL were modified by incorporating 1-vinylimidazole ligands featuring terminal double bonds that can be polymerized while exploiting the amine function of the ligand to coordinate to the nickel metal ion. A similar approach has been used successfully to produce UV curable SPME PIL coatings featuring silver ion for the selective extraction of unsaturated compounds [28].

In the current study, the following three types of SPME sorbent coatings were prepared: (1) polymerized neat $[\text{Ni}^{2+}(\text{VIM})_4] 2[\text{NTf}_2^-]$ monomer (PIL 1), (2) $[\text{Ni}^{2+}(\text{VIM})_4] 2[\text{NTf}_2^-]$ monomer with the addition of 50% w/w of $[(\text{VIM})_2\text{C}_{12}^{2+}] 2[\text{NTf}_2^-]$ as cross-linker (PIL 2), and (3) $[\text{HVIM}^+][\text{NTf}_2^-]$ monomer and a cross-linker (PIL 3). The goal was to investigate the effect of added cross-linker (PIL 1 vs. PIL 2) and the presence of nickel cation (PIL 2 vs. PIL 3) on the extraction performance for a variety of amines. The chemical structures and physical properties of the fiber coatings are shown in Table 1.

As the analytes should be released from the fiber by thermal desorption, the thermal stability of PIL sorbent coating is very important. The fibers were tested by exposure to the GC inlet. All PIL fibers were stable up to 200°C. In comparison, nonpolymerized ILs with the same anion and containing Ni^{2+} ion showed significantly lower decomposition temperatures of 164 and 178°C, respectively [22]. It can be concluded that the increased thermal resistance in the tested coatings results from the formation of a stable polymer structure [35].

The visual appearance, thickness, and regularity of the developed nickel-based PIL sorbent coatings were evaluated using SEM. Figure 2 shows the images of fibers with and without added cross-linker.

3.2 | Optimization of the extraction procedure

When optimizing extraction methods in SPME, the most important parameters are extraction and desorption times, sampling and desorption temperatures, salt concentration, and sample agitation. In the case of compounds that dissociate in aqueous solutions, sample solution pH should also be taken into account.

Amines are weak bases and can undergo hydrolysis in aqueous solutions. To facilitate their transfer to the HS, they must remain undissociated. Thus, the pH of the aqueous samples must be adjusted accordingly. The pK_a values describing acidity of protonated amines are listed in Supporting Information Table S1. Tripropylamine lies at the upper limit with a pK_a equal to 10.58. According to the general rule of equilibrium, it is widely accepted that keeping the pH of the solution two units above the pK_a value of analytes ensures its quantitative presence in the neutral

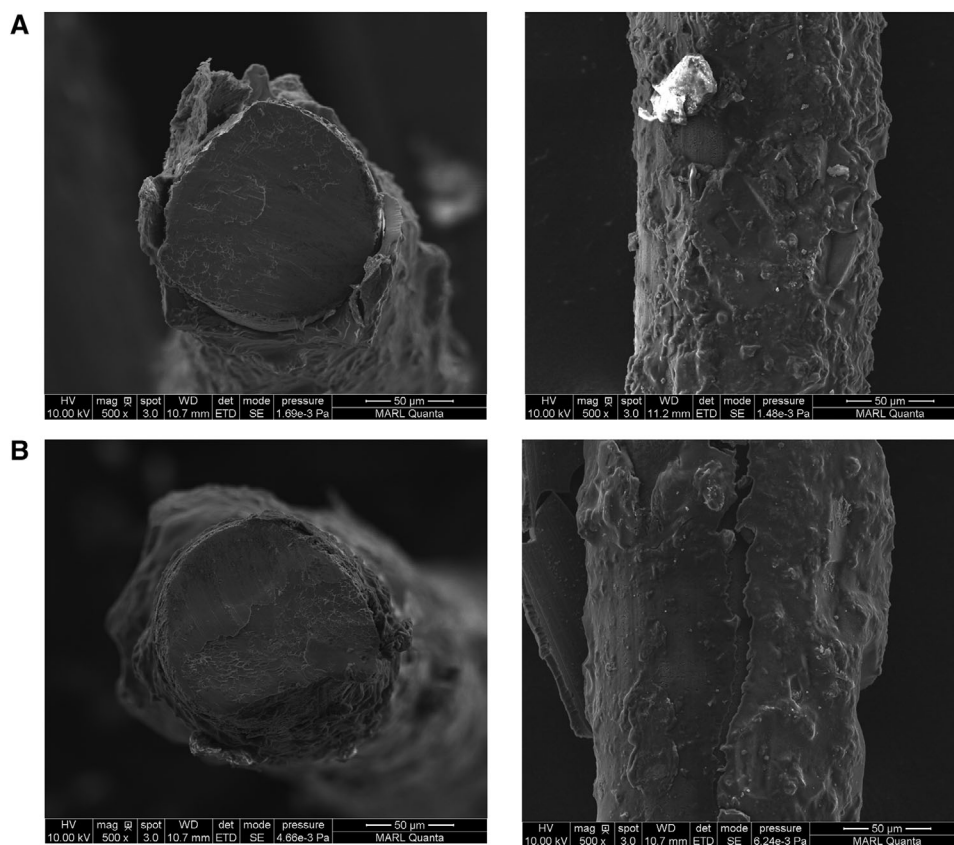


FIGURE 2 Scanning electron microscopy (SEM) images of the nickel-based PIL fibers examined in this study: PIL 1 (500 \times) $\approx 8 \pm 1.3 \mu\text{m}$ (A) and PIL 2 (500 \times) $\approx 11 \pm 1.9 \mu\text{m}$ (B)

form [36]. Therefore, the pH of the aqueous solution was increased by the addition of a strong base (NaOH) to 13.

The values of some parameters mentioned above were assumed a priori. The thermal desorption temperature of the analytes should permit their quickest possible transfer to the chromatographic column. Typically, the limitation is the thermal stability of the sorbent material and analytes. Based on the previously determined durability of the fibers (approximately 200°C), it was assumed that analytes could still be desorbed at a slightly lower temperature of 190°C.

The optimal time for thermal desorption was determined using a pre-determined temperature of the GC injection port. For optimization purposes, extraction of analytes using the tested fibers was carried out from samples using a concentration two times higher than the planned working range (i.e., 400 $\mu\text{g/L}$). The desorption studies were carried out using times ranging from 2 to 20 min. The longest desorption time of 10 min was required for PIL 1 to avoid carry-over effects. To ensure uniform conditions for all investigated fibers, the identical desorption time was applied in all further experiments.

Stirring using a magnetic stir bar was utilized as the sample agitation method. It is well known that increasing agitation of the sample is often accompanied by an increase

in the mass transfer caused by convection [5]. In this study, the highest stirring speed was limited by the formation of droplets of samples on the fiber surfaces caused by too vigorous agitation. Thus, as optimal stir rate of 800 rpm was used for all experiments in the study.

3.2.1 | Influence of salt content

Previous HS-SPME studies reported that the addition of salts can affect the extraction efficiency due to the salting out effect [37]. The interaction of water with these additional ions may have a significant impact on the extraction process as their solubility in water can be expected to increase or decrease. Amines may be particularly susceptible to the salting out effect [5]. Since the change in solubility of analytes in water is related to the sample HS equilibrium, the salting out effect was investigated with fibers containing the PIL 1 and PIL 2 sorbent coatings. Aqueous samples that did not contain NaCl yielded very low extraction efficiency and high experimental error (RSD > 15%). Hence, NaCl concentrations of 5, 15, and 30% (w/v) were evaluated at 40°C with an extraction time of 30 min. The obtained results are shown in Supporting Information

Figure S6. The results indicate that in the case of the tested amines, the addition of salt significantly reduced their solubility in water and increased their extraction efficiency from the HS. The most pronounced effect was observed for pyridine using PIL 1 where the chromatographic peak area increased by 44-fold; in contrast, the extraction efficiency for 2,6-DTBP using PIL 2 increased only by twofold. For the analyzed analytes, the effect of NaCl addition was qualitatively and quantitatively similar for both PIL 1 and PIL 2. Based on obtained results, solutions with a concentration of 30% (w/v) were chosen for further experiments.

3.2.2 | Influence of extraction temperature

It is known that an increase in the extraction temperature often leads to an increase in the diffusion coefficient, thereby increasing the rate of mass transfer to the HS [5]. The effect of extraction temperature on the extraction efficiency was investigated in the temperature range from 25 to 70°C (in 15°C increments) for 30 min using 30% (w/v) NaCl in the aqueous sample solution. The obtained extraction temperature profiles are shown in Supporting Information Figure S7 of SM. In the case of the HS mode, an equilibrium is formed for the analyte between the aqueous solution, HS, and sorbent coating. Partitioning of the analytes between the solution and the fiber depends on the values of the partition coefficients between the sample and the HS as well as the HS and fiber coating. As can be observed, the extraction efficiency evolves with increasing temperature in four ways: reaches a maximum (3-ethylpyridine, pyridine), decreases (triallylamine, 2,6-DTBP), increases (tripropylamine), and remains constant (aniline). Increasing extraction temperature may also impede analyte absorption on sorbents because of it being an exothermic process [38]. A decreasing trend in extraction efficiency for volatile analytes (i.e., triallylamine, 2,6-DTBP, and pyridine) at higher temperatures is likely due to their absorption on PIL sorbents being more hindered compared to the case of less volatile analytes at the given conditions. The profiles obtained for both fibers (PIL 1 and PIL 2) follow a similar trend, except for tripropylamine, where in the case of the cross-linked sorbent coating the extraction efficiency increases significantly with temperature. A compromised temperature condition of 45°C was identified and chosen for all amines.

3.2.3 | Influence of extraction time

The optimal extraction time was determined by analyzing the analyte extraction efficiency upon exposing the fiber to the sample HS at times varying from 10 to 70 min

using an extraction temperature of 45°C and 30% (w/v) NaCl in the aqueous sample solution. Supporting Information Figure S8 shows the effect of extraction time on the extraction efficiency of PIL 1 and PIL 2 sorbent coatings. It can be observed that for different analytes, various trends were obtained. For aniline and 2,6-DTBP, the extraction efficiency did not change significantly when extraction times longer than 10 min were tested. Pyridine, tripropylamine, and 3-ethylpyridine were more efficiently extracted at longer extraction times, while a drop in extraction efficiency occurred for triallylamine.

There is no single physicochemical property that explains the differences in time profiles obtained for different analytes as the most volatile analyte (pyridine) does not reach equilibrium in the tested time range, while the least volatile 2,6-DTBP undergoes equilibration after 10 min. Also, it could be expected that for compounds with higher values of the enrichment factor (EF) their transport within the fiber coating will require an extended equilibration time. Meanwhile, triallylamine shows even a slight decrease in extraction efficiency in PIL 2 with time, while the less efficiently extracted tripropylamine is far from equilibrium. In determining the optimal extraction time, the compounds that did not reach equilibrium within the studied time (tripropylamine, 3-ethylpyridine, and pyridine) were taken into account. For those compounds, extending the extraction time from 50 to 70 min increased the sum of chromatographic peaks areas by less than 20%. Thus, in further studies, an extraction time of 50 min was used for all fibers.

3.3 | Analytical performance of the developed HS-SPME method and evaluation of extraction efficiency

Partial validation of the HS-SPME method utilizing the PIL and commercial fibers involved determination of coefficient of determination (R^2), LODs, LOQs, repeatability (RSD), and relative recovery (RR). The working ranges for all amines and each of the investigated SPME fibers are presented in Supporting Information Table S2. A working range from 5 to 200 $\mu\text{g/L}$ was used for the studied PIL and commercial fibers. For all fibers within the working range, satisfactory linearity with the R^2 values above 0.990 was found (see Supporting Information Table S2). Supporting Information Table S3 shows the sensitivities of the methods expressed by the calibration slope for each fiber. In the case of most amines (with the exception of 2,6-DTBP), the nickel-based fibers (PIL 1 and PIL 2) exhibited higher sensitivity than commercial fibers and the PIL 3 fiber.

The LODs were calculated on the basis of an S/N of 3, and the LOQs as ten times the above-mentioned ratio.

TABLE 2 LOD (S/N = 3) and RSD obtained for amines when performing HS-SPME-GC-MS using different SPME fibers. LOD determined using samples spiked to 5 and 50 $\mu\text{g/L}$. RSD calculated using results obtained for samples with a concentration of analytes equal to 200 $\mu\text{g/L}$

Analyte	LOD ^a ($\mu\text{g/L}$)					RSD ^c (%) ($n = 3$)				
	PIL 1	PIL 2	PIL 3	PDMS_100	PA ^b	PIL 1	PIL 2	PIL 3	PDMS_100	PA
Pyridine	0.70	0.22	1.41	0.56	7.21	7.9	5.2	13.4	7.8	13.6
Triallylamine	0.28	0.03	0.01	0.08	3.19	11.1	13.4	14.7	6.0	11.9
Tripropylamine	0.24	0.02	0.04	0.27	n.d.	14.7	4.3	11.9	6.2	n.d.
3-Ethylpyridine	0.05	0.09	0.78	0.30	1.02	12.6	7.7	10.3	2.6	5.9
Aniline	1.56	0.84	1.11	6.48 ^b	1.82	8.8	14.0	13.9	5.8	6.2
2,6-DTBP	0.003717	0.000077	0.000295	0.000022	0.000072	13.9	13.6	13.1	10.8	11.4

^a5 $\mu\text{g/L}$: the spiked concentration of amines.

^b50 $\mu\text{g/L}$: the spiked concentration of amines.

n.d. – not detected.

^c200 $\mu\text{g/L}$: the spiked concentration of amines.

The LOD values of 2,6-DTBP for all fibers were significantly lower compared to other amines with a maximum of 0.0037 $\mu\text{g/L}$ for PIL 1 and a minimum of 0.000077 $\mu\text{g/L}$ for PIL 2. LODs of the other amines ranged from 0.05 to 1.56 $\mu\text{g/L}$ for PIL 1, 0.02 to 0.84 $\mu\text{g/L}$ for PIL 2, 0.01 to 1.41 $\mu\text{g/L}$ for PIL 3, 1.02 to 12.76 $\mu\text{g/L}$ for PA, and 0.08 to 6.48 $\mu\text{g/L}$ for PDMS (Table 2). LODs of pyridine, triallylamine, tripropylamine, and aniline obtained with the PIL-based SPME method were similar to or lower than the LOD values measured with other analytical methods such as capillary electrophoresis, GC-MS, and dispersive liquid–liquid microextraction coupled with GC-MS, which ranged from 0.07 to 42 $\mu\text{g/L}$ [39–42]. The LOQ values for all fibers are shown in Supporting Information Table S4.

The repeatability of the methods was calculated by performing triplicate extractions of aqueous samples spiked with amines at a concentration 200 $\mu\text{g/L}$, and are presented in Table 2. The RSD values for PIL fibers did not exceed 15% for all analytes and are comparable with those obtained using commercial fibers. RR was calculated as the ratio of the concentrations of spiked solutions to its value determined in the course of the analytical procedure. Calculated RR values are summarized in Supporting Information Table S5. The RRs ranged from 84.5 to 116.3% for all fibers, proving the usefulness of the PIL fibers in analytical applications. The performance of each type of PIL fiber began to decrease after ~70 extraction/desorption cycles. Therefore, 60 cycles was selected as the optimal lifetime of the sorbent coatings.

In addition, a comparison was made between the extraction efficiency of the developed nickel-based PIL fibers and selected commercial fibers (PA and 100 μm PDMS) using the EF [43]. This parameter is a suitable tool for comparing the extraction ability by considering the nature of the sorption coatings of fibers, regardless of its geometrical dimensions. The EF parameter was calculated as the ratio

of the analyte concentration in the fiber and the analyte concentration in the aqueous sample. The obtained values of EFs are shown in Supporting Information Table S6 and represented in Figure 3. An example chromatogram is shown in Supporting Information Figure S9. The EF values for both nickel-based PIL fibers (PIL 1 and PIL 2) are higher than those obtained for the both commercial fibers (PA and PDMS) and standard PIL fiber (PIL 3) in the case of all target analytes, with the exception of 2,6-DTBP for the PIL 1 fiber. For most analytes, the EF values of PIL 2 were higher than PIL 1. This is due to the increased surface area of the cross-linked PIL 2 resulting in enhanced analyte–sorbent interactions [44, 45]. Therefore, the PIL 2 fiber was most suitable for the extraction of amines by HS-SPME in this work. This sorbent coating may be a particularly attractive alternative to commercially available coatings for the determination of volatile amines.

3.4 | Analysis of real samples

Lake and tap water were analyzed to evaluate the matrix effect of environmental samples on the performance of the developed nickel-based PIL fibers and the HS-SPME-GC-MS method for the determination of amines. The water samples were spiked with amines at a concentration of 200 $\mu\text{g/L}$ and extracted under optimal conditions using the PIL 1 and PIL 2 fibers. The matrix effect was evaluated in terms of RR and repeatability (Table 3). The RRs of lake water ranged from 84.8 to 112.4% for PIL 1 and from 79.2 to 119.3% for PIL 2. For spiked tap water samples, the RRs varied between 90.9 and 120.0% for PIL 1 and 83.0 and 122.7% for PIL 2. The obtained RSD values for both fibers and both types of water samples were acceptable and were less than 15%. Based on both parameters, no significant matrix effects were identified.

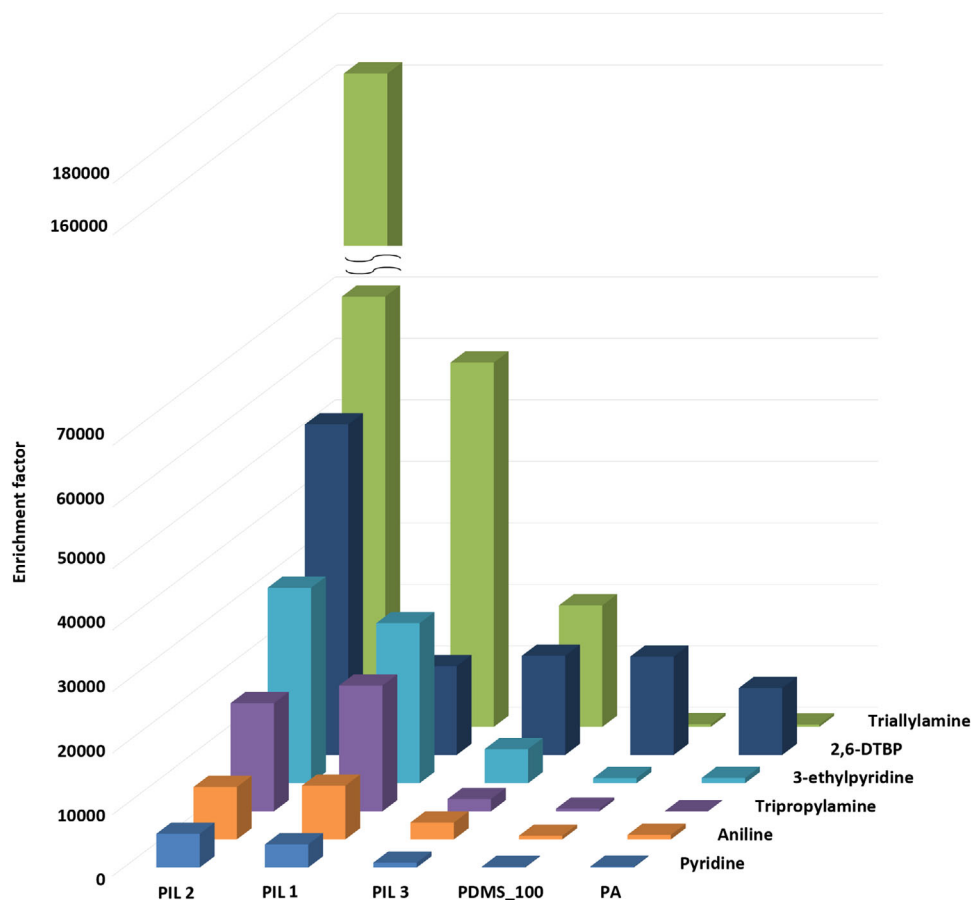


FIGURE 3 Enrichment factors calculated for the studied amines using five different SPME fibers featuring highly varied sorbent coating chemistries

TABLE 3 Analysis of lake and tap water using the HS-SPME-GC-MS method with nickel-based PIL fibers

Analyte	PIL 1				PIL 2			
	Lake water		Tap water		Lake water		Tap water	
	RR (%)	RSD (%)	RR (%)	RSD (%)	RR (%)	RSD (%)	RR (%)	RSD (%)
Pyridine	112.4	3.0	99.3	12.1	119.3	8.2	105.6	5.0
Triallylamine	99.4	10.9	118.9	11.4	82.5	12.9	122.2	4.8
Tripropylamine	87.7	5.5	120.0	6.0	98.3	5.7	98.3	9.7
3-Ethylpyridine	108.3	12.9	90.9	6.7	118.7	8.4	122.7	4.2
Aniline	111.9	6.2	107.3	12.5	91.0	14.0	93.8	10.5
2,6-DTBP	84.8	10.9	114.1	10.0	79.2	8.5	83.0	12.4

4 | CONCLUDING REMARKS

In this work, two nickel-based PIL sorbent coatings were successfully developed and applied in HS-SPME coupled to GC-MS for the determination of volatile and semivolatile amines, including pyridine, triallylamine, tripropylamine, 3-ethylpyridine, aniline, and 2,6-DTBP, from water samples. After optimizing the extraction parameters, the extraction efficiency of the developed fibers (PIL 1 and PIL 2) was evaluated and compared with commercial fibers using the EF normalization parameter.

The nature of the nickel-based sorbent coatings provided higher efficiencies than the conventional PIL coating as well as commercial PA and PDMS coatings for all of the analytes studied.

Additionally, the results from this study show that the analytical performance of the nickel-based PIL, PA, and PDMS (100 μm) fibers were comparable in terms of working range, coefficient of determination, LOD, LOQ, reproducibility, and RR. Low LODs were achieved for developed fibers, and ranged from 0.003717 to 1.56 mg/L and from 0.000077 to 0.84 $\mu\text{g/L}$ for PIL 1 and PIL 2,

respectively. Finally, the developed HS-SPME-GC-MS method was applied for the analysis of real samples, including tap and lake water. The RRs of PIL 2 ranged from 83.0 to 122.7% for tap water and from 79.2 to 119.3% for lake water.

ACKNOWLEDGMENTS

J.L.A. acknowledges funding from the Chemical Measurement and Imaging Program at the National Science Foundation (Grant No. CHE-1709372). Kateryna Yavir acknowledges the development of an interdisciplinary Ph.D. program with an international dimension (InterPhD II, POWR.03.02.00-IP.08-00-DOK/16) for the funding provided to carry out the following research.


CONFLICT OF INTEREST

The authors have declared no conflict of interest.

ORCID

Kateryna Yavir  <https://orcid.org/0000-0002-6274-609X>

Adam Kloskowski  <https://orcid.org/0000-0003-4342-5837>

Jared L. Anderson  <https://orcid.org/0000-0001-6915-8752>

REFERENCES

- Kataoka H. Derivatization reactions for the determination of amines by gas chromatography and their applications in environmental analysis. *J Chromatogr A*. 1996;733:19–34.
- Zhu Y, Wang MH, Du HY, Wang F, Mou SF, Haddad PR. Organic analysis by ion chromatography: 1. Determination of aromatic amines and aromatic diisocyanates by cation-exchange chromatography with amperometric detection. *J Chromatogr A*. 2002;956:215–20.
- Chung KT. Mutagenicity and carcinogenicity of aromatic amines metabolically produced from azo dyes. *Environ Carcinog Revs*. 2000;C18:51–74.
- Arthur CL, Pawliszyn J. Solid phase microextraction with thermal desorption using fused silica optical fibers. *Anal Chem*. 1990;62:2145–8.
- Pawliszyn J. *Handbook of Solid Phase Microextraction*. Waltham, MA: Elsevier; 2012.
- Kataoka H, Lord HL, Pawliszyn J. Applications of solid-phase microextraction in food analysis. *J Chromatogr A*. 2000;880:35–62.
- Chary NS, Fernandez-Alba AR. Determination of volatile organic compounds in drinking and environmental waters. *Trends Anal Chem*. 2012;32:60–75.
- Snow NH. Solid-phase micro-extraction of drugs from biological matrices. *J Chromatogr A*. 2000;885:445–55.
- Hashemi B, Zohrabi P, Shamsipur M. Recent developments and applications of different sorbents for SPE and SPME from biological samples. *Talanta*. 2018;187:337–47.
- Yu H, Ho TD, Anderson JL. Ionic liquid and polymeric ionic liquid coatings in solid-phase microextraction. *Trends Anal Chem*. 2013;45:219–32.
- Patinha DJ, Silvestre AJ, Marrucho IM. Poly (ionic liquids) in solid phase microextraction: Recent advances and perspectives. *Prog Polym Sci*. 2019;98:101148.
- Yavir K, Marcinkowski Ł, Marcinkowska R, Namieśnik J, Kloskowski A. Analytical applications and physicochemical properties of ionic liquid-based hybrid materials: A review. *Anal Chim Acta*. 2019;1054:1–16.
- Gutiérrez-Serpa A, Rocío-Bautista P, Pino V, Jiménez-Moreno F, Jiménez-Abizanda AI. Gold nanoparticles based solid-phase microextraction coatings for determining organochlorine pesticides in aqueous environmental samples. *J Sep Sci*. 2017;40:2009–21.
- Luo Z, Chen G, Li X, Wang L, Shu H, Cui X, Chang C, Zeng A, Fu Q. Molecularly imprinted polymer solid-phase microextraction coupled with ultra high performance liquid chromatography and tandem mass spectrometry for rapid analysis of pyrrolizidine alkaloids in herbal medicine. *J Sep Sci*. 2019;42:3352–62.
- Li G, Row K. Ternary deep eutectic solvent magnetic molecularly imprinted polymers for the dispersive magnetic solid-phase microextraction of green tea. *J Sep Sci*. 2018;41:3424–31.
- Wan Ibrahim WN, Sanagi MM, Mohamad Hanapi NS, Kamaruzaman S, Yahaya N, Wan Ibrahim WA. Solid-phase microextraction based on an agarose-chitosan-multiwalled carbon nanotube composite film combined with HPLC–UV for the determination of nonsteroidal anti-inflammatory drugs in aqueous samples. *J Sep Sci*. 2018;41:2942–51.
- Abolghasemi MM, Yousefi V, Piryaei M. Synthesis of a metal-organic framework confined in periodic mesoporous silica with enhanced hydrostability as a novel fiber coating for solid-phase microextraction. *J Sep Sci*. 2015;38:1187–93.
- Zeeuw J, Vonk N, Buyten J, Heijnsdijk P, Clarisse R. *The Analysis of Volatile Amines by Capillary Gas Chromatography*. Middelburg, the Netherlands: Varian; 2000.
- Qian W, Texter J, Yan F. *Frontiers in poly(ionic liquid)s: synthesis and applications*. *Chem Soc Rev*. 2017;46:1124–59.
- Yuan J, Mecerreyes D, Antonietti M. Poly(ionic liquid)s: an update. *Prog Polym Sci*. 2013;38:1009–36.
- Mei M, Huang X, Chen L. Recent development and applications of poly (ionic liquid)s in microextraction techniques. *Trends Anal Chem*. 2019;112:123–34.
- Chand D, Farooq MQ, Pathak AK, Li J, Smith EA, Anderson JL. Magnetic ionic liquids based on transition metal complexes with N-alkylimidazole ligands. *New J Chem*. 2019;43:20–3.
- Santos E, Albo J, Irabien A. Magnetic ionic liquids: synthesis, properties and applications. *RSC Adv*. 2014;4:40008–18.
- Wang H, Yan R, Li Z, Zhang X, Zhang S. Fe-containing magnetic ionic liquid as an effective catalyst for the glycolysis of poly (ethylene terephthalate). *Catal Commun*. 2010;11:763–7.
- Sajid M. Magnetic ionic liquids in analytical sample preparation: a literature review. *Trends Anal Chem*. 2019;113:210–23.
- Clark KD, Nacham O, Purslow JA, Pierson SA, Anderson JL. Magnetic ionic liquids in analytical chemistry: a review. *Anal Chim Acta*. 2016;934:9–21.
- Nan H, Peterson L, Anderson JL. Evaluating the solvation properties of metal-containing ionic liquids using the solvation parameter model. *Anal Bioanal Chem*. 2018;410:4597–606.
- Trujillo-Rodríguez MJ, Anderson JL. Silver-based polymeric ionic liquid sorbent coatings for solid-phase microextraction:

- Materials for the selective extraction of unsaturated compounds. *Anal Chim Acta*. 2019;1047:52–61.
29. Ho TD, Yu H, Cole WT, Anderson JL. Ultraviolet photoinitiated on-fiber copolymerization of ionic liquid sorbent coatings for headspace and direct immersion solid-phase microextraction. *Anal Chem*. 2012;84:9520–8.
 30. Anderson JL, Armstrong DW. Immobilized ionic liquids as high-selectivity/high-temperature/high-stability gas chromatography stationary phases. *Anal Chem*. 2005;77:6453–62.
 31. Anderson JL, Ding R, Ellern A, Armstrong DW. Structure and properties of high stability geminal dicationic ionic liquids. *J Am Chem Soc*. 2005;127:593–604.
 32. Ho TD, Toledo BR, Hantao LW, Anderson JL. Chemical immobilization of crosslinked polymeric ionic liquids on nitinol wires produces highly robust sorbent coatings for solid-phase microextraction. *Anal Chim Acta*. 2014;843:18–26.
 33. Yu H, Merib J, Anderson JL. Faster dispersive liquid–liquid microextraction methods using magnetic ionic liquids as solvents. *J Chromatogr A*. 2016;1463:11–9.
 34. Chisvert A, Benedé JL, Anderson JL, Pierson SA, Salvador A. Introducing a new and rapid microextraction approach based on magnetic ionic liquids: Stir bar dispersive liquid microextraction. *Anal Chim Acta*. 2017;983:130–40.
 35. Pierson SA, Nacham O, Clark KD, Nan H, Mudryk Y, Anderson JL. Synthesis and characterization of low viscosity hexafluoroacetylacetonate-based hydrophobic magnetic ionic liquids. *New J Chem*. 2017;41:5498–505.
 36. Sarafraz-Yazdi A, Ardaki MS, Amiri A. Determination of monocyclic aromatic amines using headspace solid-phase microextraction based on sol–gel technique prior to GC. *J Sep Sci*. 2013;36:1629–35.
 37. Vila M, Celeiro M, Lamas JP, Dagnac T, Llompart M, Garcia-Jares C. Determination of fourteen UV filters in bathing water by headspace solid-phase microextraction and gas chromatography-tandem mass spectrometry. *Anal Methods*. 2016;8:7069–79.
 38. Sarafraz-Yazdi A, Vatani H. A solid phase microextraction coating based on ionic liquid sol–gel technique for determination of benzene, toluene, ethylbenzene and o-xylene in water samples using gas chromatography flame ionization detector. *J Chromatogr A*. 2013;1300:104–11.
 39. Hattori T, Okamura H, Asaoka S, Fukushi K. Capillary zone electrophoresis determination of aniline and pyridine in sewage samples using transient isotachopheresis with a system-induced terminator. *J Chromatogr A*. 2017;1511:132–7.
 40. Liu S, Wang W, Chen J, Sun J. Determination of aniline and its derivatives in environmental water by capillary electrophoresis with on-Line concentration. *Int J Mol Sci*. 2012;13:6863–72.
 41. Tsukioka T, Ozawa H, Murakami T. Gas chromatographic-mass spectrometric determination of lower aliphatic tertiary amines in environmental samples. *J Chromatogr A*. 1993;642:395–400.
 42. Diao CP, Wei CH. Rapid determination of anilines in water samples by dispersive liquid–liquid microextraction based on solidification of floating organic drop prior to gas chromatography–mass spectrometry. *Anal Bioanal Chem*. 2012;403:877–84.
 43. Pena-Pereira F, Marcinkowski Ł, Kloskowski A, Namiesnik J. Silica-based ionogels: nanoconfined ionic liquid-rich fibers for headspace solid-phase microextraction coupled with gas chromatography–barrier discharge ionization detection. *Anal Chem*. 2014;86:11640–8.
 44. Trujillo-Rodríguez MJ, Nan H, Anderson JL. Expanding the use of polymeric ionic liquids in headspace solid-phase microextraction: Determination of ultraviolet filters in water samples. *J Chromatogr A*. 2018;1540:11–20.
 45. Ho TD, Yu H, Cole WTS, Anderson JL. Ultraviolet photoinitiated on-fiber copolymerization of ionic liquid sorbent coatings for headspace and direct immersion solid-phase microextraction. *Anal Chem*. 2012;84:9520–8.

SUPPORTING INFORMATION

Additional supporting information may be found online in the Supporting Information section at the end of the article.

How to cite this article: Yavir K, Eor P, Kloskowski A, Anderson JL. Polymeric metal-containing ionic liquid sorbent coating for the determination of amines using headspace solid-phase microextraction. *J Sep Sci*. 2021;44:2620–2630.
<https://doi.org/10.1002/jssc.202100119>